Detection of cerebral microbleeds with venous connection at 7 Tesla MRI

Johanna Rotta, MD^{1*}, Valentina Perosa, MD^{1,2,3*}, Renat Yakupov, MSc^{2,4}, Hugo J Kuijf, PhD⁵, Frank Schreiber, MSc^{1,4}, Laura Dobisch, MSc⁴, Jan Oltmer, MD², Anne Assmann, MD¹, Oliver Speck, PhD^{4,6,7,8}, Hans-Jochen Heinze, MD^{1,2,4,6,7}, Julio Acosta-Cabronero, PhD⁹, Emrah Düzel, MD^{2,4,6,7,10}, Stefanie Schreiber, MD^{1,4,7}

- ¹ Department of Neurology, Otto-von-Guericke University, Magdeburg, Germany
- ² Institute of Cognitive Neurology and Dementia Research (IKND), Magdeburg, Germany
- ³ J. Philip Kistler Stroke Research Center, Massachusetts General Hospital, Boston, USA
- ⁴ German Center for Neurodegenerative Diseases (DZNE), Magdeburg, Germany
- ⁵ Image Sciences Institute, University Medical Center Utrecht, Utrecht, The Netherlands
- ⁶ Leibniz-Institute for Neurobiology (LIN), Magdeburg, Germany
- ⁷ Center for behavioral brain sciences (CBBS), Magdeburg, Germany
- ⁸ Institute of Physics, Otto-von-Guericke University, Magdeburg, Germany
- ⁹ Tenoke Limited, Cambridge, UK
- ¹⁰ Institute of Cognitive Neuroscience, University College London, London, UK

* Both authors contributed equally to this work.

Paper: 2989 words Abstract: 230 words Title: 71 characters Number of references: 50 Number of figures: 3 Number of tables: 3 Search terms: 7 Tesla MRI [120], cerebral small vessel disease (CSVD) [13], cerebral amyloid angiopathy (CAA) [13], microbleeds [7], quantitative susceptibility mapping (QSM) [120]

Corresponding author: Valentina Perosa, MD J. Philip Kistler Stroke Research Center, Massachusetts General Hospital Cambridge Str. 175, Suite 300 Boston, MA 02114, USA Tel: +1 8572631663 Fax: +1 617-726-5043 VPEROSA@mgh.harvard.edu

Johanna Rotta and Valentina Perosa conducted the statistical analysis at Otto-von-Guericke University, Department of Neurology, Leipziger Str. 44, 39102 Magdeburg, Germany (J.R) and Massachusetts General Hospital, Cambridge Str. 175, Boston, MA 02114, USA (V.P.).

Study funding: Supported by the BMBF (EnergI-Consortium, TP01) and the German Research Foundation, CRC 779 (TP A07).

The study has not been supported by any sponsor.

The authors report no disclosures/conflicts of interest.

ORCID iDs

Valentina Perosa 0000-0002-3551-5237

Hugo J Kuijf 0000-0001-6997-9059

Frank Schreiber 0000-0002-9484-8613

Oliver Speck 0000-0002-6019-5597

Julio Acosta-Cabronero 0000-0003-1174-5983

Emrah Düzel 0000-0002-0139-5388

Stefanie Schreiber 0000-0003-4439-4374

Abstract Objective: Cerebral microbleeds (MBs) are a common finding in cerebral small vessel disease (CSVD) and Alzheimer's disease patients as well as in healthy elderly people, but their pathophysiology remains unclear. To investigate a possible role of veins in hat formatiert: Hervorheben the development of MBs, we performed an exploratory study, to assess in vivo presence of MBs with a direct connection to a vein. We conducted this exploratory Kommentiert [JR1]: Recently, we added an additional requirement related to structured abstracts. In the Objective section, please add one sentence to state the tudy to determine for the first time in vive whether there is a spatial connection hypothesis ('e.g., to determine whether') followed by the means by which it was tested. Example: Objective: To petween small veins and MBs in different CSVD subgroups and controls. Methods: 7 test the hypothesis that all frogs are made from cells, we dissected 42,000 frogs and performed histology on 5 organs, assuming this is as an adequate sample for Tesla (7 T) MRI was conducted and MBs were counted on Quantitative Susceptibility generalizability. hat formatiert: Hervorheben Mapping (QSM). A submillimeter resolution QSM-based venogram allowed identification of lobar, deep and infratentorial-MBs with a direct spatial connection to a vein. Results: 51 subjects (mean age[SD] 70.5[8.6] years, 37% females) participated hat formatiert: Hervorheben in the study -20 were patients with CSVD (Cerebral Amyloid Angiopathy (CAA) with strictly lobar MBs (n=8), hypertensive Arteriopathy (HA) with strictly deep MBs (n=5), and mixed lobar and deep MBs (n=7), mean age [SD]-72.4-[6.1] vears, 30-% females) and 31<u>were</u> healthy controls (mean age [SD] 69.4-[9.9] <u>years</u>, 42-% females)-were ncluded in the study (whole sample: 51 subjects (mean age [SD] 70.5 [8.6], 37 % Kommentiert [JR2]: 1) In the abstract and the text, please include the number of the enrolled participants, as well as their demographic characteristics (including females). In our cohort, wWe counted a total of 96 MBs with a venous connection-in for the whole sample) in the results section and not in the methods our cohort, representing 14-% of all detected MBs on 7T QSM. Most venous MBs (86%, n = 83) were observed in lobar locations and all of these were cortical. CAA subjects showed the highest ratio of venous to total MBs (19%).... Conclusions: Our findings Kommentiert [PV3]: @Johanna, please add... establish a link between cerebral MBs and the venous vasculature, pointing towards a possible contribution of veins to CSVD in general and to CAA in particular. Pathological studies are needed to confirm our observations.

Rotta 3

Abbreviations

Aß	Amyloid-beta
AD	Alzheimer's disease
BBB	Blood-brain barrier
BG	Basal ganglia
BW	receiver bandwidth
CAA	Cerebral Amyloid Angiopathy
CSO	Centrum semiovale
cSS	cortical superficial siderosis
CSVD	Cerebral Small Vessel Disease
FA	Flip angle
GRAPPA	Generalized autocalibrating partial parallel acquisition
HA	Hypertensive Arteriopathy
ICH	Intracerebral hemorrhage
MBs	O a walk walk was held a site
	Cerebral microbleeds
MSDI	Cerebral microbleeds Multi-Scale Dipole Inversion
-	
MSDI	Multi-Scale Dipole Inversion
MSDI MRI	Multi-Scale Dipole Inversion Magnetic Resonance Imaging
MSDI MRI PVS	Multi-Scale Dipole Inversion Magnetic Resonance Imaging Perivascular spaces
MSDI MRI PVS QSM	Multi-Scale Dipole Inversion Magnetic Resonance Imaging Perivascular spaces Quantitative Susceptibility Mapping
MSDI MRI PVS QSM SWI	Multi-Scale Dipole Inversion Magnetic Resonance Imaging Perivascular spaces Quantitative Susceptibility Mapping Susceptibility Weighted Imaging

Introduction

Cerebral microbleeds (MBs) are small hypointense round lesions, visible on T2*-weighted magnetic resonance imaging (MRI) and susceptibility weighted imaging (SWI). They are a hallmark of cerebral small vessel disease (CSVD), which affects cerebral vessels smaller than 1 mm and causes hemorrhagic and ischemic stroke, dementia, gait impairment¹ and represents an increasingly recognized contributing factor to Alzheimer's (AD) and further neurodegenerative diseases². The most common forms of sporadic CSVD are cerebral amyloid angiopathy (CAA),

which mainly affectings the leptomeningeal and cortical small arteries, and hypertensive arteriopathy (HA) of the deep perforating arteries^{3,4}. The distribution and number of MBs, which is lobar in CAA, deep (thalamus, basal ganglia) in HA^{5,6} or mixed (lobar and deep)^{7,8} aids in the stratification of the individual risk for intracerebral hemorrhage (ICH)⁹.

Histopathological correlation studies claim that the majority of MBs seen on MRI are acute, subacute or chronic small focal lesions of accumulating intact erythrocytes or hemosiderin^{10,11} resulting from leakage or rupture of a small vessel. The predominant pathological involvement of arterioles and small arteries in CSVD¹² thereby suggests that MBs mainly derive from the arterial tree¹³. However, cortical and leptomeningeal venous β -amyloid- β (Aß)-accumulation has been observed in both animal models of

-	Kommentiert [JR4]: Shorten the Introduction to 250
	words.
	-Wir haben aktuell 460 Wörter.

Kommentiert [PV5R4]: I gave it a try. Jetzt sind es 252. -Ich habe den Aspekt der high resolution zur Diskussion geschoben und die genaue objectives rausgeloescht.

- -Ich habe auch die "Wichtigkeit" von CSVD nicht mehr ewaehnt.
- -Nicht so huebsch, aber ich denke es funktioniert auch so.

Kommentiert [PV6]: Bitte in einer formattieren (wie 3.4)

CAA and AD¹⁴ and in human CAA^{15,16}. Further, vFurther, evidence of venous collagenosis, which is defined as the thickening of the venous vessel wall through accumulation of collagen, has was been found observed in ageing¹⁷, CSVD¹⁴ and preclinical AD models¹⁸. Therefore, a role of small veins in the development of MBs, through leakage or rupture, caused by CSVD-related venous pathology is also conceivable.

So far, pathological and *in-vivo* studies have not aimed to distinguish between<u>assess</u> venous and arterial contribution to the formation of MBs. We analyzed quantitative susceptibility mapping (QSM)-based venograms at submillimeter resolution in a cohort of CSVD patients and elderly controls to examine for the first time *in vivo* the relationship between small veins and MBs. This is in part due to the technical difficulties in detecting small veins (and arteries) at widely available 1.5 Tesla (T) and 3T MRI¹⁹. A possible way of depicting small veins is the use of high-resolution Quantitative Susceptibility Mapping (QSM) at 7T MRI. QSM is a postprocessing method, able to quantify magnetic susceptibility²⁰ and allowing MBs detection with higher sensitivity than SWI²¹. Simultaneously, QSM enables a precise visualization of the brain's venous vasculature²². Additionally, high resolution MRI leads to better visibility of small structures, while given the same resolution, scanning at high field MRI increases signal-to-noise ratio.

We analyzed submillimeter resolution 7T QSM-based venograms in a cohort of CSVD patients (CAA, HA and mixed MBs) and elderly controls to examine for the first time *in vive* the relationship between small veins and MBs. We aimed to determine (i) if there is a direct connection between small veins and MBs, to then (ii) identify the topographical localization of MBs with venous connection, and (iii) relate them to

Kommentiert [PV7]: @Johanna: bitte Barnes et al 2009 hinzu

Kommentiert [JR8R7]: Ich habe schon 50 References, mehr sind leider nicht erlaubt

certain CSVD subgroups. The present approach will shed more light on the pathophysiology of MBs in small vessel disease.

Methods

Participants

A total of 51 older adults (mean age [SD] 70.5 [8.6], 37 % females) were included in this 7T brain MRI study. The scans of this 7T brain MRI study were acquired between December 2016 2018. and July CSVD subjects Twenty of the participants (mean age [SD] 72.4 [6.1], 30 % females) suffered from CSVD and were recruited from a longitudinal 3T MRI study on the pathophysiology of CSVD conducted by the University Clinic of Magdeburg and German Center for Neurodegenerative Disease (DZNE), Magdeburg. Inclusion criteria for the 3T study was the presence of hemorrhagic CSVD markers, i.e. MBs, ICH and/or cortical superficial siderosis (cSS) on iron-sensitive MRI sequences (gradient recalled echo [GRE] T2*-weighted or susceptibility weighted imaging [SWI]) of a clinical 1.5T MRI conducted for diagnostic work-up. Clinical MRI prior inclusion was performed for several diagnostic reasons, including headache, epileptic seizures, gait disturbances, cognitive impairment and transient ischemic attack (for further details see Perosa et aP3.). CSVD participants were classified through the distribution of MBs on 3T SWI MRI as CAA, according to the modified Boston criteria, HA (strictly deep MBs) or mixed lobar and deep MBs^{4,7,24}. Thirty-one participants were considered as controlsControls were considered as such as they had no hemorrhagic markers (MBs, ICH, cSS) on 3T MRI (mean age [SD] 69.4 [9.9], 42 % females); they and were recruited from an already existing pool of cognitively normal community-dwelling elderly study participants of the

Rotta 7

Formatiert: Block

DZNE, Magdeburg. Regarding further CSVD MRI features, in controls only white matter hyperintensities (WMH) up to grade 1 (mild) on the Fazekas visual rating scale²⁵ and grade 1 perivascular spaces (PVS) in the basal ganglia (BG) or centrum semiovale (CSO) were allowed because they represent a common finding in aging²⁶.

Cardiovascular risk factors were additionally recorded for all participants (Table 1). Arterial hypertension was identified when blood pressure exceeded 130/80 mmHg. Diabetes mellitus was diagnosed as fasting plasma glucose level > 7.0 mmol/L or 11.1 mmol/L two hours after glucose tolerance test. Hyperlipidemia was defined as abnormal blood levels of low-density lipoprotein cholesterol (> 2.6 mmol/L) and/or triglycerides (> 1.7 mmol/L). Genetic neurological disease, history of psychiatric disease, alcohol or drug abuse, as well as cerebrovascular malformations were excluded in all participants. None of the subjects included in our study presented clinical (headache, altered conscious state, nausea) or neuroimaging signs (e.g. edema, hemorrhagic venous infarction, engorged cortical and transmedullary veins) of cerebral venous thrombosis. Likewise, an inspection of the 7T SWI images was negative with respect to the same markers, also in all the visible small veins. Contraindications for scanning at 7T, according to the recommendations of the German Ultrahigh Field Imaging network, were considered and represented a further exclusion criterion from our study.

Standard Protocol Approvals, Registrations, and Patient Consents

The study was approved by the local Ethics Committee (93/17; 28/16). All participants provided written informed consent according to the declaration of Helsinki and were compensated for travel costs.

MRI acquisition at 7T MRI

Kommentiert [JR9]: In a subsection within your Methods labeled "Standard Protocol Approvals, Registrations, and Patient Consents", please state that you:

a.Received approval from an ethical standards committee on human experimentation (institutional or regional) for any experiments using human subjects; If there was a waiver from your institution's ethical approval board, please note the waiver in this section and provide documentation to the editorial office that waiver was granted.

b.Received written informed consent was obtained from all patients (or guardians of patients) participating in the study (consent for research).

c.Provided the identity of the public trials registry and the clinical trial identifier number (if applicable).

d.Obtained authorization for disclosure (consent-todisclose) of any recognizable persons in photographs, videos, or other information that may be published in the Journal, in derivative works by the AAN, or on the Journal's Web site (when applicable).

Rotta 8

MRI acquisition was conducted on a high-field 7T MRI (Siemens Healthineers, Erlangen) equipped with a 32-channel head-coil (Nova Medical, Wilmington). SWI acquisition was conducted with a voxel size of 0.35 x 0.35 x 1.5 mm³ in a 3D GRE sequence. The acquisition parameters were as follows: echo time (TE) 9 ms, repetition time (TR) 18 ms, flip angle (FA) 10°, receiver bandwidth (BW) 100 Hz/pixel, 3D matrix dimensions 200 x 169 x 132. GRAPPA (generalized autocalibrating partial parallel acquisition) was enabled with an acceleration factor of 2 and 32 reference lines. The T1-weighted sequence with 3D magnetization-prepared rapid gradient echo (3D-MPRAGE) was acquired with a voxel size of 1 x 1 x 1 mm³ and the following parameters: TE 2.89ms, TR 2250 ms, FA 5°, inversion time 1050 ms, BW 130 Hz/pixel, echo spacing 8.3 ms, 3D matrix dimensions 256 x 256 x 176; GRAPPA was enabled 3 32 with acceleration factor and reference lines The protocol included more sequences that were not used in our study. Total scanning time was 50 minutes.

7T MRI QSM reconstruction

In order to calculate quantitative susceptibility maps, which allow the generation of the brain venogram and depiction of MBs, the acquired complex SWI data underwent the following reconstruction steps. First, multiple-channel complex image data were combined using an adaptive algorithm²⁷ followed by automatic reference channel selection. The combined phase data were then unwrapped using a continuous Laplacian approach²⁸. Adopting FSL's BET routing (threshold 0.1), a brain mask was calculated from the magnitude image and applied to the phase image. Then, the background field was removed in two steps: Laplacian boundary value (LBV)²⁹ with two-layer region of interest (ROI)-peeling, followed by variable mean spherical value (vSMV)³⁰ with r0 = 40 mm and step size/final kernel radius of 1 mm. Finally, a Multi-

Scale Dipole Inversion (MSDI)²² was carried out in order to reconstruct quantitative susceptibility maps from the local field maps obtained in the previous step. This reconstruction algorithm provides high specificity for venous blood susceptibilities.

Count of MBs with and without venous connection

MBs were defined as hyperintense, round lesions of up to 5 mm in the QSM reconstruction. For verification, their appearance was matched on the SWI sequence where MBs are hypointense and associated with a blooming effect³¹ (Figure 1). According to the Microbleed Anatomical Rating Scale (MARS)³², MBs were counted in lobar (frontal, parietal, temporal, occipital, insular), deep (deep and periventricular white matter, basal ganglia, thalamus, internal capsule, external capsule and corpus callosum) and infratentorial (brainstem, cerebellum) regions separately, and additionally summed up (i.e. whole-brain number of MBs, MBtot). The localization of lobar MBs was additionally distinguished as cortical, if they were located within the cortex, or non-cortical.

MBs with a direct link to a vein were assessed in the QSM sequence. They were defined as "MBs with venous connection" (MBven) if the connection was visible at least on one slice (Figure 2A). Number and localization (lobar [cortical, non-cortical], deep, infratentorial, total) were recorded using the same approach described in the previous paragraph. To double check the spatial relationship between small veins and MBs on 7T QSM images, MBs and the venogram were visualized in 3 dimensions applying MeVisLab Version 3.1.1 (MeVis, Bremen, Germany) 2B). (Figure In lobar, deep, infratentorial and total regions, we further determined the ratio between MBs with venous connection and all MBs (MBven/MBtot) in the respective region, hereby calculating the ratio of venous MBs detected MBs. to all

Kommentiert [PV10]: @Johanna: Here please add REF by Liu et al 2012

In all 51 subjects, number of MBs was counted by two independent raters (J.R. 2 years of experience; V.P. 5 years of experience). Interrater reliability was very good to excellent (intraclass correlation coefficient for SWI 0.96, for QSM 0.86). Presence and localization of MBven was assessed in consensus by the same raters, disagreement rate was low (< 10%). All visual image analysis was performed on MRIcron (CNRL, University of South Carolina, USA).

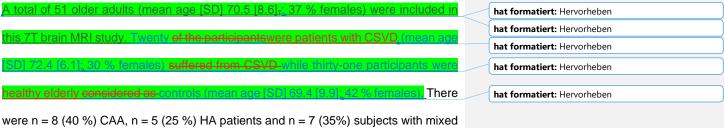
Data Availability

De-identified data are available from the corresponding author upon reasonable request subject to a material transfer agreement.

Statistics

We applied Kruskal-Wallis test with Dunn-Bonferroni post-hoc test to evaluate group differences (controls, CAA, HA, mixed MBs) for the respective number of lobar, deep, infratentorial and total (i) MBs, (ii) MBven (iii) MBven/MBtot. Statistical analyses were two-tailed and conducted using the Statistical Package for Social Science (IBM SPSS Statistics), version 23.

Results



were n = 8 (40 %) CAA, n = 5 (25 %) HA patients and n = 7 (35%) subjects with mixed MBs. All groups were comparable with regard to age and sex. CSVD patients (all

subgroups) had a higher prevalence of arterial hypertension compared to controls (Table 1).

The use of 7T QSM allowed to observe at least one MB in 80% (n = 25) of the healthy elderly controls. The finding is remarkable, given the fact that none of the control subjects presented MBs on the baseline 3T MRI (see inclusion criteria of healthy controls). Considering that the repercussion on the classification into the different groups, based on the additional MBs detected applying 7T QSM, was not the aim of our study, we maintained the classification based on the baseline 3T MRI. Both, CAA (Mdn=15.5) and mixed MBs subjects (Mdn=16) presented more MBtot than controls (Mdn=1) (Dunn-Bonferroni post-hoc tests: p < 0.001, r = 0.64 and p = 0.002, r = 0.59 respectively). As expected, the number of lobar MBs was higher in CAA (Mdn=11.5) than in HA (Mdn=0) and controls (Mdn=1) (p = 0.006, r = 0.91 and p < 0.001, r = 0.65); the number of lobar MBs was higher in mixed MBs subjects (Mdn=10) than in controls (Mdn=1) (p = 0.024, r = 0.47); the number of deep MBs was higher in mixed MBs subjects (Mdn=4) compared to controls (Mdn=0) (p = 0.006, r = 0.53); the number of infratentorial MBs was higher in mixed MBs subjects (Mdn=4) than in CAA (Mdn=0) and controls (Mdn=0) (p = 0.006, r = 0.53); the number of infratentorial MBs was higher in mixed MBs subjects (Mdn=4) compared to controls (Mdn=0) (p = 0.006, r = 0.53); the number of infratentorial MBs was higher in mixed MBs subjects (Mdn=4) than in CAA (Mdn=0) and controls (Mdn=0) (p = 0.006, r = 0.53); the number of infratentorial MBs was higher in mixed MBs subjects (Mdn=4) than in CAA (Mdn=0) and controls (Mdn=0) (p = 0.002, r = 0.80 and p < 0.001, r = 0.82).

In our cohort, we counted a total of n = 96 MBven, representing 14 % of all detected MBs on 7T QSM (n = 674). N = 19 (37%) of all subjects showed MBven, including n = 7 CAA (88% of all CAA cases), n = 2 HA (40%), n = 7 mixed MBs (100%) patients and n = 3 controls (10%). The prevalence of MBven in MB-presenting controls was consequently 12% (3/25). The vast majority of MBven (87%, n = 83) were observed in lobar locations, and all of them were cortical. CAA patients (Mdn= 3.5) showed significantly more lobar MBven than controls (Mdn=0) (r = 0.57, p = 0.002, r = 0.57) (Table 2). Also, subjects with mixed MBs (Mdn=2) presented significantly more lobar

Kommentiert [JR11]: Habe hier im Text darauf verzichtet, jedes Mal die range mit anzugeben (aus Gründen der Leserlichkeit und weil am Ende alles in einem Satz und zusätzlich in Table 2 zusammengefasst ist)

Kommentiert [PV12R11]: Ok, as long as that meets the journal's criteria. I think it does

Kommentiert [PV13]: How can the median be 3.5???

MBven than controls (Mdn=0) (p < 0.001, r = 0.76) and HA subjects (r = 0.85, p = 0.020; r=0.85). Only n = 5 (5%) and n = 8 (8%) of MBven were found in deep and infratentorial regions, respectively (Table 2 and -) (Table-3). In each group, m Median (range) of total MBven number, and mean [SD] MBven/MBtot was 3.5 (0-23) and 19% [15] in CAA, 0 (0-1) and 9% [14] in HA, 2 (1-13) and 18% [15] in mixed MBs, and 0 (0-1) and 5% [20] in controls, resulting in significant group differences (Mdn, H(3) = 29.73, p < 0.001. Mean and H(3) = 21.33, p < 0.001, respectively). Post-hoc tests revealed that number of total MBven and MBven/MBtot was higher in CAA and mixed MBs compared to controls (for MBven: r = 0.63, p < 0.001; r = 0.72, p < 0.001, and for MBven/MBtot: r = 0.54, p = 0.005; r = 0.62, p = 0.001, respectively), with no differences between the remaining groups (Figure 3; Table 2). We detected a total of 3 MBvon in controls. Consequently, the

Kommentiert [JR14]: Dieser Satz stand schon zuvor so drin, war aber wohl nicht ausreichend raw data. Würde es dann so (doppelt) drinlassen. Kommentiert [PV15]: Again...ich denke nicht dass es possible ist hat formatiert: Hervorheben Kommentiert [JR16]: Hier habe ich nicht noch einmal die raw data in Klammern dahintergesetzt, da sie ja im Satz davor beschrieben sind. Für euch annehmbar?

Kommentiert [JR18]: Rauslassen oder an einer anderen Stelle?

Kommentiert [PV17R16]: Ja!

Discussion

This high-resolution 7T neuroimaging study investigated if a spatial relationship between small veins and MBs could be detected in a cohort of CSVD patients. QSM enabled depiction of cerebral MBs with a direct connection to a vein and their localization. These lesions accounted for 14% of all MBs. Our data support the notion that MBs might not exclusively derive from arteries, but that venous contribution could play an important, yet not much explored, role in MBs and - presumably - CSVD pathogenesis. Venous collagenosis, for example, leads to thickening of the walls of small cerebral veins³³. This could result in increased luminal pressure and leakage of the blood-brain barrier (BBB), a pivotal mechanism of CSVD and (maybe) MB initiation^{34–36}. Venous collagenosis further relates to the development of WMH³⁷ and lacunes¹⁸. In line with this, in CSVD, a semiguantitative visual score

created to assess pathological changes of the deep medullary veins was also independently associated with WMH volume³⁸ and presence of multiple MBs³⁹. A direct relationship between a vein and a MB has also previously been observed in a 7 T MRI study⁴⁰. However, to date, no dedicated studies have been carried out in order to distinguish between MBs of arterial and venous origin¹⁰.

The distribution of MBs with venous connection in our study was predominantly lobar (87% of all venous MBs) and all of these MBs were located in the cortex. Conversely, only 5% of all venous MBs were found in deep, and 8% in infratentorial regions. Furthermore, CAA patients presented the highest ratio of venous MBs to total MBs (19%). These findings <u>could</u> suggest a relation to CAA pathology, in that the association between small veins and MBs could involve vascular Aß-pathology⁴¹ or the related vessel wall remodelling⁴². However, other pathological mechanisms might play a role as well. Unfortunately, pathological studies that investigated MBs so far have not systematically distinguished whether the ruptured vessel was a vein or an artery¹⁰. Setting a focus on presence and kind of venous pathology in CSVD in general, and in CAA in particular, can have important repercussions on our understanding of clearance pathways in the human brain – While the hypothesis of clearance through the

ueber die Clearance pathways geloescht: Das Thema ist so am entwickeln und nach den ganzen diskussionen an der iCAA conference und hier in Boston denke ich, dass wir uns damit zu sehr aus dem Fenster lehnen...

Kommentiert [PV19]: @Steffi: Ich habe Genaueres

A major strength of our study is the use of high-resolution QSM at 7T MRI, which conveys high sensitivity for MB detection⁴⁵. High-resolution MRI leads to better visibility of small structures, while given the same resolution, scanning at high field MRI increases signal-to-noise ratio. QSM is a postprocessing method²⁰, which allows MBs

Kommentiert [PV20]: @Johanna: bitte Barnes et al 2009 hinzu

detection with higher sensitivity than SWI²¹. Simultaneously, QSM enables a precise visualization of the brain's venous vasculature²². In particular, t₁-As QSM — compared to SWI - removes the blooming effect⁴⁶, we can exclude the possibility that the connection we see between small veins and MBs is due to this artifact. Furthermore, not only QSM is an innovative reconstruction technique, but also the high-resolution used in this study enabled visualization of small veins. The MSDI algorithm adopted for QSM reconstruction²² provides in fact—high specificity for venous blood susceptibilities, making it highly unlikely that we measured arterioles or small arteries with slow blood flow instead. <u>As QSM – compared to SWI - removes the blooming</u> effect⁴⁶, we can also exclude the possibility that the connection we see between small veins and MBs is due to this artifact. Moreover, higher sensitivity and reliability of SWI compared to T2*-weighted GRE MRI in the detection of MBs and veins, suggest that the observation of MBs with a venous connection would not benefit from the use of the latter.

Previous studies that matched ex-vivo ultra-high resolution MRI with the corresponding pathological changes¹¹ showed that increasing resolution and field-strength in MRI not only allowed to detect more MBs, but also non-hemorrhagic vasculopathic changes. One might therefore argue that what we observed are not MBs of venous origin but vasculopathic changes, such as microaneurysms. However, at a similar MRI resolution (voxel size: 0.2 mm³ isotropic) as in our study, -(voxel size: 0.2 mm³ isotropic) 90% of all detected susceptibility artifacts were confirmed to be hemorrhagic lesions in pathology¹¹.

It is thought that the majority of cortical MBs originate from medullary arteries in CAA. The combined use of ultra-high resolution time of flight angiography⁴⁷ (down to a voxel size of 0.15 mm³) and of a QSM derived venogram could allow to observe "leaky" Kommentiert [PV21]: @Johanna: please readd here ref 21 (Kohls et al, I think), Barnes et al 2009.

cortical arteries as concurring vessel of origin of the MBs. At present, we cannot completely rule out the possibility that the spatial relationship that we observe is not a causal one. Only_<u>patho</u>histo<u>pathol</u>logical correlation studies specifically targeting venous MBs can confirm the nature of these lesions and shed further light on the role of veins in CSVD.

The main limitation of our study is the small size of the cohort. However, this needs to be set into relation with the difficulties of acquiring 7T MRI, which has several contraindications, especially when taking into account account of an elderly hospital-based population suffering from vascular disease. In fact, previous studies adopting 7T MRI in similar cohorts were not larger^{48–50}. For the same reasons, a selection bias towards healthier participants that do not mirror the full spectrum of CSVD, might have occurred. Despite the predictable higher sensitivity at submillimeter resolution 7T MRI, detection of MBs of venous origin is also possible using QSM at 3T (authors' observation), which can allow to broaden the number of study's participants in the future.

To our best knowledge, this is the first human neuroimaging study to systematically investigate the spatial relation between cerebral small veins and MBs in-vivo. Our findings establish a link between the venous microvasculature and, especially lobar, cerebral MBs, highlighting the role of small veins in CSVD, particularly suggesting a link to CAA pathology. Deepening the knowledge on these lesions could convey new insight into CSVD.

Acknowledgements

We are very grateful to all participants who volunteered to take part in the study. We thank Anna Ludwig and Denver Huff for help in subject recruitment and data collection.

We also wish to thank Renate Blobel-Lüer, Claus Tempelmann, Hendrik Mattern and Daniel Stucht for their dedicated efforts in scanning standardisation and quality assurance.

		Rotta 16	
Name	Location	Contribution	+ Formatierte Tabelle
Johanna Rotta, MD	Otto-von-Guericke University, Magdeburg, Germany	Study design; analyzed the data; drafted manuscript for intellectual content	Formatiert: Rechts: 2,5 cm, Unten: 2 cm, Breite: 21 cm, Höhe: 29,7 cm
Valentina Perosa, MD	Massachusetts General Hospital, Boston, USA	Study design; analyzed the data; drafted manuscript for intellectual content	
Renat Yakupov, MSc	German Center for Neurodegenerative Diseases (DZNE), Magdeburg, Germany	Processed part of the data; revised the manuscript for intellectual content	
Hugo J Kuijf, PhD	University Medical Center Utrecht, the Netherlands	Revised the manuscript for intellectual content	
Frank Schreiber, MSc	Otto-von-Guericke University, Magdeburg, Germany	Processed part of the data; revised the manuscript for intellectual content	
Laura Dobisch, MSc	German Center for Neurodegenerative Diseases (DZNE), Magdeburg, Germany	Visualized the data; revised the manuscript for intellectual content	
Jan Oltmer, MD	Otto-von-Guericke University, Magdeburg, Germany	Visualized the data; revised the manuscript for intellectual content	
Anne Assmann, MD	Otto-von-Guericke University, Magdeburg, Germany	Revised the manuscript for intellectual content	
Oliver Speck, PhD	Otto-von-Guericke University, Magdeburg, Germany	Revised the manuscript for intellectual content	
Hans-Jochen Heinze, MD	Otto-von-Guericke University, Magdeburg, Germany	Revised the manuscript for intellectual content	
Julio Acosta- Cabronero, MSc	Tenoke Limited, Cambridge, United Kingdom	Revised the manuscript for intellectual content	

Emrah Düzel, MD	German Center for Neurodegenerative Diseases (DZNE), Magdeburg, Germany	Revised the manuscript for intellectual content
Stefanie Schreiber, MD	Otto-von-Guericke University, Magdeburg, Germany	Study design; analyzed the data; drafted manuscript for intellectual content
Appendix 1: Authors		

Kommentiert [JR22]: Jetzt portrait statt landscape format

hat formatiert: Hervorheben

References

1. Shi Y, Wardlaw JM. Update on cerebral small vessel disease: a dynamic wholebrain disease. Stroke Vasc Neurol. 2016;1(3):83–92.

2. Greenberg SM, Bacskai BJ, Hernandez-Guillamon M, Pruzin J, Sperling R, van Veluw SJ. Cerebral amyloid angiopathy and Alzheimer disease - one peptide, two pathways. Nat Rev Neurol. 2020;16:30–42.

3. Martinez-Ramirez S, Greenberg SM, Viswanathan A. Cerebral microbleeds: overview and implications in cognitive impairment. Alzheimers Res Ther. 2014;6:33.

4. Greenberg SM, Charidimou A. Diagnosis of Cerebral Amyloid Angiopathy: Evolution of the Boston Criteria. Stroke 2018;49:491–497.

5. Fazekas F, Kleinert R, Roob G, et al. Histopathologic Analysis of Foci of Signal Loss on Gradient-Echo T2*-Weighted MR Images in Patients with Spontaneous Intracerebral Hemorrhage: Evidence of Microangiopathy-Related Microbleeds. Am J Neuroradiol. 1999;20:637–642.

6. Linn J, Halpin A, Demaerel P, et al. Prevalence of superficial siderosis in patients with cerebral amyloid angiopathy. Neurology 2010;74:1346–1350.

7. Pasi M, Charidimou A, Boulouis G, et al. Mixed-location cerebral hemorrhage/microbleeds: Underlying microangiopathy and recurrence risk. Neurology 2018;90:e119-e126.

8. Smith EE, Romero JR. Mixed emotions: What to do with patients who have lobar and deep hemorrhages on MRI? Neurology 2018;90:55–56.

9. Wermer MJH, Greenberg SM. The growing clinical spectrum of cerebral amyloid angiopathy. Curr Opin Neurol. 2018;31:28–35.

10. Shoamanesh A, Kwok CS, Benavente O. Cerebral microbleeds: histopathological correlation of neuroimaging. Cerebrovasc Dis. 2011;32:528–534.

11. van Veluw SJ, Charidimou A, van der Kouwe AJ, et al. Microbleed and microinfarct detection in amyloid angiopathy: a high-resolution MRI-histopathology study. Brain 2016;139:3151–3162.

12. Wu Y, Chen T. An Up-to-Date Review on Cerebral Microbleeds. J Stroke Cerebrovasc Dis. 2016;25:1301–1306.

13. Fisher M, French S, Ji P, Kim RC. Cerebral microbleeds in the elderly: a pathological analysis. Stroke 2010;41:2782–2785.

14. Klakotskaia D, Agca C, Richardson RA, Stopa EG, Schachtman TR, Agca Y. Memory deficiency, cerebral amyloid angiopathy, and amyloid- β plaques in APP+PS1 double transgenic rat model of Alzheimer's disease. PLoS ONE. 2018;13:e0195469.

15. Weller RO, Boche D, Nicoll JAR. Microvasculature changes and cerebral amyloid angiopathy in Alzheimer's disease and their potential impact on therapy. Acta Neuropathol. 2009;118:87–102.

16. Mendel T, Wierzba-Bobrowicz T, Stępień T, Szpak GM. β-amyloid deposits in veins in patients with cerebral amyloid angiopathy and intracerebral haemorrhage. Folia Neuropathol. 2013;51:120–126.

17. Moody DM, Brown WR, Challa VR, Ghazi-Birry HS, Reboussin DM. Cerebral microvascular alterations in aging, leukoaraiosis, and Alzheimer's disease. Ann N Y Acad Sci. 1997;826:103–116.

18. Keith J, Gao F-Q, Noor R, et al. Collagenosis of the Deep Medullary Veins: An Underrecognized Pathologic Correlate of White Matter Hyperintensities and Periventricular Infarction? J Neuropathol Exp Neurol. 2017;76:299–312.

19. Bouvy WH, Kuijf HJ, Zwanenburg JJM, et al. Abnormalities of Cerebral Deep Medullary Veins on 7 Tesla MRI in Amnestic Mild Cognitive Impairment and Early Alzheimer's Disease: A Pilot Study. J Alzheimers Dis. 2017;57:705–710.

20. Haacke EM, Liu S, Buch S, Zheng W, Wu D, Ye Y. Quantitative susceptibility mapping: current status and future directions. Magn Reson Imaging. 2015;33:1–25.

21. Klohs J, Deistung A, Schweser F, et al. Detection of cerebral microbleeds with quantitative susceptibility mapping in the ArcAbeta mouse model of cerebral amyloidosis. J Cereb Blood Flow Metab. 2011;31:2282–2292.

22. Acosta-Cabronero J, Milovic C, Mattern H, Tejos C, Speck O, Callaghan MF. A robust multi-scale approach to quantitative susceptibility mapping. NeuroImage 2018;183:7–24.

23. Perosa V, Priester A, Ziegler G, et al. Hippocampal vascular reserve associated with cognitive performance and hippocampal volume. Brain 2020;143(2):622-634.

24. Tsai H-H, Tsai L-K, Chen Y-F, et al. Correlation of Cerebral Microbleed Distribution to Amyloid Burden in Patients with Primary Intracerebral Hemorrhage. Sci Rep. 2017;7:44715.

25. Fazekas F, Chawluk JB, Alavi A, Hurtig HI, Zimmerman RA. MR signal abnormalities at 1.5 T in Alzheimer's dementia and normal aging. AJR Am J Roentgenol. 1987;149:351–356.

26. Schmidt R, Fazekas F, Kapeller P, Schmidt H, Hartung HP. MRI white matter hyperintensities: three-year follow-up of the Austrian Stroke Prevention Study. Neurology 1999;53:132–139.

27. Walsh DO, Gmitro AF, Marcellin MW. Adaptive reconstruction of phased array MR imagery. Magn Reson Med. 2000;43:682–690.

28. Schofield MA, Zhu Y. Fast phase unwrapping algorithm for interferometric applications. Opt Lett. 2003;28:1194–1196.

29. Zhou D, Liu T, Spincemaille P, Wang Y. Background field removal by solving the Laplacian boundary value problem. NMR Biomed. 2014;27:312–319.

30. Li W, Wu B, Liu C. Quantitative susceptibility mapping of human brain reflects spatial variation in tissue composition. Neuroimage 2011;55:1645–1656.

31. Wardlaw JM, Smith EE, Biessels GJ, et al. Neuroimaging standards for research into small vessel disease and its contribution to ageing and neurodegeneration. Lancet Neurol. 2013;12:822–838.

32. Gregoire SM, Chaudhary UJ, Brown MM, et al. The Microbleed Anatomical Rating Scale (MARS): reliability of a tool to map brain microbleeds. Neurology 2009;73:1759–1766.

33. Zhou Y, Li Q, Zhang R, et al. Role of deep medullary veins in pathogenesis of lacunes: Longitudinal observations from the CIRCLE study. J Cereb Blood Flow Metab. 2019;40(9):1797-1805.

34. Schreiber S, Bueche CZ, Garz C, Braun H. Blood brain barrier breakdown as the starting point of cerebral small vessel disease? - New insights from a rat model. Exp Transl Stroke Med. 2013;5:4.

35. Wardlaw JM, Makin SJ, Valdés Hernández MC, et al. Blood-brain barrier failure as a core mechanism in cerebral small vessel disease and dementia: evidence from a cohort study. Alzheimers Dement. 2017;13(6):634–643.

36. Freeze WM, Jacobs HIL, Jong JJ de, et al. White matter hyperintensities mediate the association between blood-brain barrier leakage and information processing speed. Neurobiol Aging. 2020;85:113–122.

37. Black S, Gao F, Bilbao J. Understanding white matter disease: imagingpathological correlations in vascular cognitive impairment. Stroke. 2009;40(3 Suppl):48-52.

38. Zhang R, Zhou Y, Yan S, et al. A Brain Region-Based Deep Medullary Veins Visual Score on Susceptibility Weighted Imaging. Front Aging Neurosci. 2017;9:269.

39. Zhang R, Li Q, Zhou Y, Yan S, Zhang M, Lou M. The relationship between deep medullary veins score and the severity and distribution of intracranial microbleeds. Neuroimage Clin. 2019;23:101830.

40. Kuijf HJ, Bresser J de, Geerlings MI, et al. Efficient detection of cerebral microbleeds on 7.0 T MR images using the radial symmetry transform. NeuroImage 2012;59:2266–2273.

41. Gurol ME, Dierksen G, Betensky R, et al. Predicting sites of new hemorrhage with amyloid imaging in cerebral amyloid angiopathy. Neurology 2012;79:320–326.

42. van Veluw SJ, Scherlek AA, Freeze WM, et al. Different microvascular alterations underlie microbleeds and microinfarcts. Ann Neurol. 2019;86:279–292.

43. Rasmussen MK, Mestre H, Nedergaard M. The glymphatic pathway in neurological disorders. The Lancet Neurology 2018;17:1016–1024.

44. van Veluw SJ, Reijmer YD, van der Kouwe AJ, et al. Histopathology of diffusion imaging abnormalities in cerebral amyloid angiopathy. Neurology 2019;92:e933-e943.

45. Bresser J de, Brundel M, Conijn MM, et al. Visual cerebral microbleed detection on 7T MR imaging: reliability and effects of image processing. AJNR Am J Neuroradiol. 2013;34:E61-E64.

46. Wang Y, Liu T. Quantitative susceptibility mapping (QSM): Decoding MRI data for a tissue magnetic biomarker. Magn Reson Med. 2015;73:82–101.

47. Mattern H, Sciarra A, Godenschweger F, et al. Prospective motion correction enables highest resolution time-of-flight angiography at 7T. Magn Reson Med. 2018;80:248–258.

48. Conijn MMA, Geerlings MI, Biessels G-J, et al. Cerebral microbleeds on MR imaging: comparison between 1.5 and 7T. AJNR Am J Neuroradiol. 2011;32:1043–1049.

49. Brundel M, Heringa SM, Bresser J de, et al. High prevalence of cerebral microbleeds at 7Tesla MRI in patients with early Alzheimer's disease. J Alzheimers Dis. 2012;31:259–263.

50. Springer E, Dymerska B, Cardoso PL, et al. Comparison of Routine Brain Imaging at 3 T and 7 T. Invest Radiol. 2016;51:469–482.

Tables

	CAA (n = 8)	HA (n = 5)	Mixed MBs (n = 7)	Controls (n = 31)	Group differences
Age years	71.6 [+/- 7.5]	76.4 [+/- 2.1]	70.3 [+/- 5.4]	69.4 [+/- 9.9]	H(3) = 3.93, p = 0.27
Female %	50	0	29	42	H(3) = 3.96, p = 0.27
BMI kg/m²	26.8 [+/- 2.4]	26.3 [+/- 4.8]	27.8 [+/- 3.9]	25.2 [+/- 2.4]	H(3) = 4.51, p = 0.21
Diabetes mellitus %	13	40	43	10	H(3) = 5.92, p = 0.12
Arterial hypertension %	100	80	100	52	H(3) = 10.42, p = 0.015 post-hoc tests not significant
Hyperlipidemia %	50	80	71	39	H(3) = 4.20, p = 0.24

Table 1. Characteristics of groups. The table reports the characteristics of the study participants, including demographics and vascularriskfactors.Ifnotstatedotherwise,meanandSDaregiven.Kruskal-Wallistestisreported.Key:BMI:body mass index;CAA:cerebral amyloid angiopathy;HA:hypertensive angiopathy;MBs = microbleeds.

	CAA (n = 8)	HA (n = 5)	Mixed MBs (n = 7)	Controls (n = 31)	Group differences
Lobar MBs	11.5 (3-168)	0 (0-6)	10 (1-51)	1 (0-5)	H(3) = 23.34, p < 0.001 CAA/HA*, CAA/CON*, Mixed MBs/CON*
Deep MBs	0.5 (0-6)	0 (0-5)	4 (0-22)	0 (0-18)	H(3) = 11.02, p = 0.012 Mixed MBs/CON*
Infratentorial MBs	0 (0-10)	1 (0-2)	4 (1-14)	0 (0-2)	H(3) = 27.36, p < 0.001 Mixed MBs/CON*, Mixed MBs/CAA*
Total MBs (MBtot)	15.5 (4-168)	2 (1-11)	16 (2-69)	1 (0-21)	H(3) = 24.6, p < 0.001 CAA/CON*, Mixed MBs/CON*
Lobar MBven	3.5 (0-23)	0 (0-1)	2 (1-10)	0 (0-1)	H(3) = 29.67, p < 0.001 CAA/CON*, Mixed MBs/CON*, Mixed MBs/HA*
Deep MBven	0	0	0 (0-2)	0 (0-1)	H(3) = 7.92, p = 0.048 post-hoc tests ns
Infratentorial MBven	0 (0-4)	0 (0-1)	0 (0-1)	0	H(3)= 8.65, p = 0.034 post-hoc tests ns
Total MBven	3.5 (0-23)	0 (0-1)	2 (1-13)	0 (0-1)	H(3) = 29.73, p < 0.001 CAA/CON*, Mixed MBs/CON*
MBven/MBtot % mean [+/-SD]	19 [15]	9 [14]	18 [15]	5 [20]	H(3) = 21.33, p < 0.001 CAA/CON*, Mixed MBs/CON*

Table 2. Total and venous microbleeds. This table reports the number of total microbleeds (MBtot) and MBs with a venous connection (MBven) according to brain localization for each of our study's subgroup. If not stated otherwise, median and range are given. Kruskal-Wallis and post-hoc Dunn-Bonferroni test statistics are reported and highlighted bold and with an asterisk in case of significant group/subgroup differences. Key: CAA: cerebral amyloid angiopathy; HA: hypertensive arteriopathy.

Subject no	Sex	Age at 7T MRI	CSVD subgroup (based on 3T SWI)	Cortical superficial siderosis (cSS)	Intracerebral Hemorrhage (ICH)	Lobar total MBs	Deep total MBs	Infratentorial total MBs	Total MBs (MBtot)	Lobar MBs with venous connection	Deep MBs with venous connection	Infratentorial MBs with venous connection	Total MBs with venous connection (MBven)
1	F	74.8	Possible CAA			88	0	0	88	23	0	0	23
2	F	79.1	Probable CAA		Lobar ICH	6	3	0	9	3	0	0	3
3	М	76.2	Probable CAA	yes		168	0	0	168	14	0	0	14
4	М	60.3	Probable CAA			26	4	10	40	10	0	4	14
5	F	64.3	Probable CAA	<mark>yes</mark>	Lobar ICH	6	0	1	7	0	0	1	1
6	F	75.1	Probable CAA	yes		3	1	0	4	0	0	0	0
7	М	78.8	Probable CAA		Lobar ICH	10	6	2	18	0	0	0	0
8	М	64.2	Probable CAA			13	0	0	13	4	0	0	4
9	М	79.7	HA		Deep ICH	6	5	0	11	0	0	1	1
10	М	76.8	HA			0	1	0	1	0	0	0	0
11	М	74.1	HA			1	0	2	3	1	0	0	1
12	М	76.0	HA			0	0	1	1	0	0	0	0

13	М	75.3	HA	1	0	2	3	0	0	0	0
14	М	73.3	Mixed	41	22	4	67	5	2	0	7
15	М	76.6	Mixed	1	5	2	8	1	0	0	1
16	М	61.1	Mixed	45	10	14	69	10	2	1	13
17	М	72.5	Mixed	51	2	8	61	6	0	1	7
18	F	74.4	Mixed	5	4	4	13	1	0	0	1
19	F	66.5	Mixed	10	3	3	16	2	0	0	2
20	М	68	Mixed	1	0	0	1	1	0	0	1
21	М	66.5	CON	1	0	0	1	0	0	0	0
22	F	69.2	CON	2	0	0	2	0	0	0	0
23	F	81.1	CON	0	1	0	1	0	0	0	0
24	F	76.7	CON	1	0	0	1	0	0	0	0
25	М	89.4	CON	0	0	0	0	0	0	0	0
26	М	70.1	CON	2	1	0	3	0	0	0	0
27	М	78	CON	1	3	0	4	0	0	0	0
28	М	55.6	CON	0	0	0	0	0	0	0	0
29	М	78.6	CON	1	1	0	2	0	0	0	0
30	F	70.7	CON	0	2	0	2	0	0	0	0
31	F	74.8	CON	1	0	0	1	0	0	0	0
32	М	77.7	CON	1	0	0	1	1	0	0	1
33	М	75.3	CON	1	0	0	1	0	0	0	0

34	F	76.8	CON		2	0	0	2	1	0	0	1
35	F	77.2	CON		1	0	0	1	0	0	0	0
36	F	48.5	CON		1	0	0	1	0	0	0	0
37	М	71.6	CON		3	0	0	3	0	0	0	0
38	М	68.8	CON		3	3	0	6	0	1	0	1
39	F	68.3	CON		2	0	2	4	0	0	0	0
40	F	65.8	CON		0	0	0	0	0	0	0	0
41	М	62.2	CON		1	3	0	4	0	0	0	0
42	М	50.6	CON		1	0	0	1	0	0	0	0
43	М	70.3	CON		2	0	0	2	0	0	0	0
44	М	64.4	CON		0	0	0	0	0	0	0	0
45	М	69	CON		5	0	0	5	0	0	0	0
46	М	73.2	CON		0	0	0	0	0	0	0	0
47	F	45.1	CON		0	0	0	0	0	0	0	0
48	F	79.0	CON		0	1	1	2	0	0	0	0
49	М	71.2	CON		0	1	0	1	0	0	0	0
50	М	58.6	CON		2	18	1	21	0	0	0	0
51	F	65.9	CON		1	0	0	1	0	0	0	0
Σ					517	100	57	674	83	5	8	96

Table 3: Detailed information on each study's participant, including location and number of total microbleeds and microbleeds with venous connection. Key: QSM = quantitative susceptibility mapping, CSVD = cerebral small vessel disease, CAA = cerebral amyloid angiopathy, CON = control, HA = hypertensive arteriopathy, M = male, F = female, No = number, Σ = sum.

Figure Legend

Figure 1

Title: Example of the visualization of a microbleed.

Legend: Example of a microbleed on 7T SWI, depicted as a hypointense round structure (A) and on 7T QSM, where it appears hyperintense (B). The inlays respectively show an enlargement of the vision.

Figure 2

Title: Venous microbleed.

Legend: Example of a microbleed (arrow) with a direct connection to a small vein (luminal diameter of ca. 700 μ m) on 7T QSM (A). 3-dimensional visualization of the venogram of a subject with CSVD (B). One microbleed (arrow) with connection to a vein is colored in blue, while those without connection are marked in red. One example of each is also shown in the enlargement in A.

Figure 3

Title: Differences in microbleeds with venous connection between groups. Legend: (A) Violin plot showing the number of microbleeds with venous connection (MBven) in each subgroup. CAA and mixed MBs patients showed a higher number of MBven compared to controls. (B) Violin plot showing the ratio of venous to total microbleeds (MBven/MBtot) in each subgroup. CAA and mixed MBs patients showed a higher ratio compared to controls. * p < 0.05; ** = p < 0.01; *** = p < 0.001. CAA = cerebral amyloid angiopathy, CON = controls, HA = hypertensive arteriopathy.